A DFT Investigation of The Host-Guest Interactions Between Boron-Based Aromatic Systems and β-Cyclodextrin

Seyfeddine Rahali (saif.rahali@gmail.com)
Qassim University College of Science and Arts in Alrass
Youghourta Belhocine
Universite du 20 aout 1955 de Skikda
Hamza Allal
Universite du 20 aout 1955 de Skikda
Abdelaziz Bouhadiba
Universite du 20 aout 1955 de Skikda
Ibtissem Meriem Assaba
Universite du 20 aout 1955 de Skikda
Mahamadou Seydou
Universite Paris

Research Article

Keywords: β-cyclodextrin, boron-based compounds, non-covalent interactions, inclusion complexes, DFT-D3

DOI: https://doi.org/10.21203/rs.3.rs-488597/v1

A DFT investigation of the host-guest interactions between boron-based aromatic systems and β-cyclodextrin

Seyfeddine Rahali[a,b,*], Youghourta Belhocine[c], Hamza Allal[d], Abdelaziz Bouhadiba[c], Ibtissem Meriem Assaba[c], Mahamadou Seydou[e]

[a] Department of Chemistry, College of Science and Arts, Qassim University, Ar Rass, Saudi Arabia.

[b] IPEIEM, Research Unit on Fundamental Sciences and Didactics, Université de Tunis El Manar, Tunis 2092, Tunisia

[c] Department of Petrochemical and Process Engineering, Faculty of Technology, 20 August 1955 University of Skikda, P.O. Box 26, El Hadaik Road, 21000, Skikda, Algeria

[d] Department of Technology, Faculty of Technology, 20 August 1955 University of Skikda, P.O. Box 26, El Hadaik Road, 21000, Skikda, Algeria

[e] Université de Paris, ITODYS, CNRS, UMR 7086, 15 rue J-A de Baïf, F-75013 Paris, France.

Corresponding author: Dr. Seyfeddine Rahali

Email saif.rahali@gmail.com ; Phone number 00966531319550

Abstract

Density-functional theory calculations including dispersion at BLYP-D3(BJ)/def2-SVP level of theory were performed for a series of systems based on cyclodextrin complexation with boron-based aromatic compounds. Elaborated investigations were carried out using different quantum chemical parameters such as computed complexation energies, theoretical association constants and natural bond orbital (NBO) analysis. Several configurations and inclusion modes were considered in this work. The calculated complexation energies were consistent with the experimental classification of these systems on the basis of occurring interactions. Reduced density gradient (RDG) and independent gradient model (IGM) approaches determined the nature and strength of non-covalent interactions which played a central role in the formation of the complexes. Thus, phenylboronic acid (PBA) and benzoxaborole (Bxb) act mainly as hydrogen-bonded complexes with β-cyclodextrin, while mainly Van der Waals (vdW) interactions stabilize both catechol (PhBcat) and pinacol esters

of phenylboronic acid (PhBpin) complexes. The ferroceneboronic acid (FcBA) exhibits a mixture of H-bonds and vdW interactions with β-cyclodextrin.

Keywords: β-cyclodextrin, boron-based compounds, non-covalent interactions, inclusion complexes, DFT-D3

1. Introduction

In recent years, organoboron compounds have become one of the most versatile classes of heteroatom-substituted organic molecules **[1-3]**. Organoboron-based compounds and their derivatives are a class of organic molecules with several applications in various fields of chemistry such as analytical and supramolecular chemistry, catalysis, energy storage and carbon capture (H_2, CH_4, CO_2...) **[4-8]**. Indeed, boronic acids have been successfully used as catalysts, e.g, for the formation of amide bonds and enantioselective reactions **[9-12]**. Since 2005, boronic acids have been used by Omar Yaghi and his collaborators as secondary building blocks to synthesize nanoporous materials, in particular covalent organic-framework like COF-1 **[6]**.

The complexes which are based on the interaction of boric acid and its derivatives [13] with macromolecular systems such as carbohydrates have several important applications, notably in the area of drug delivery. For instance, it is reported that ferroceneboronic acid (FcBA) and its derivatives could act as electrochemical biosensors for detecting sugars [14].

Boron atom is more electropositive than carbon, and this fundamental property is exploited to the fullest in organic synthesis, becoming one of the most prominent areas of application of organoboron compounds. The mildly Lewis acidic character of the boron atom is suitable in the context of carbohydrate and fluoride sensing that is enabled by the formation of tetracoordinate borates with fluoride anions and polyols **[3, 15-19]**.

In addition to the application areas mentioned before, boronic acids are used as therapeutic agents and biological probes. The first-in-class anticancer drug bortezomib has been joined by

the recently approved antifungal tavaborole, and anti-eczema drug crisaborole, while many other boronic acid derivatives have shown promising activities in a large number of clinical and preclinical studies **[20, 21]**. In this arena, boronic acids are complexed with supramolecular structures involving inclusion complexes with cyclodextrins. These studies have resulted in new commercially available drugs which have been of great benefit **[22]**.

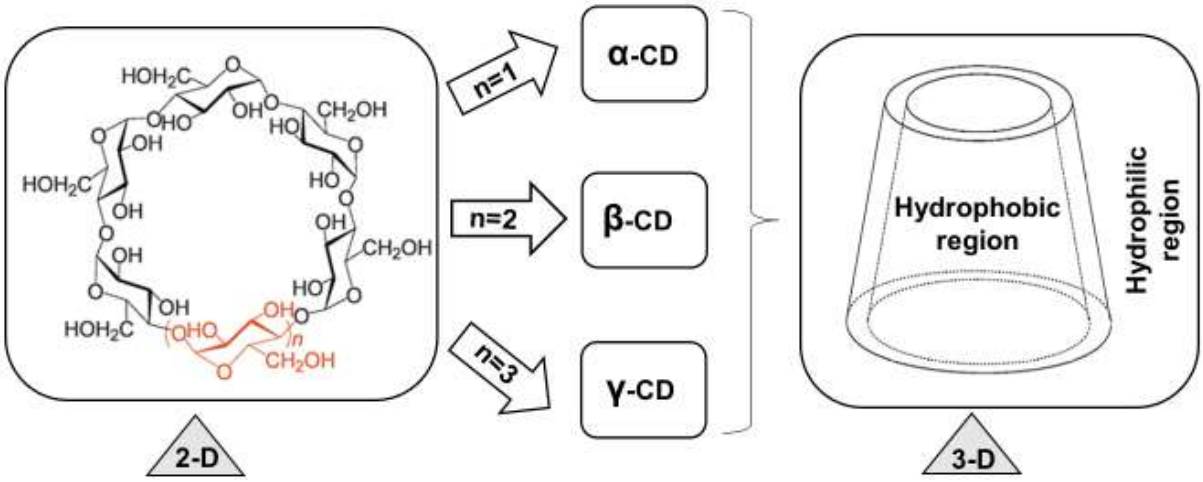

Fig. 1 Chemical structure and 3D-model of cyclodextrins.

Cyclodextrins (CDs) have been used extensively due to their advantages of non-toxicity, facile modification, good water-solubility and high biological availability. CDs have been approved as pharmaceutical excipients for the manufacture of pharmaceutical preparations. CDs are cyclic oligosaccharides formed by 6, 7 or 8 glucoses units, which are called α, β, γ-cyclodextrin respectively (See Fig. 1) **[23-25]**.

The 3D structure of CDs shows hollow truncated cone-shaped macrocycles in space, their inside cavity is hydrophobic while the outside is hydrophilic. CDs form inclusion complexes with a wide variety of boronic acids **[26-29].** In this context, Kasprzak et al. studied the interactions of some boric acid derivatives with β-cyclodextrin using spectroscopic methods: Proton nuclear magnetic resonance (^{1}H NMR), 1H Diffusion-Ordered Spectroscopy nuclear magnetic resonance (^{1}H DOSY NMR) and Fourier-transform infrared spectroscopy

(FTIR)**[30]**. They found that phenylboronic acid (PBA) and benzoxaborole (Bxb) form non-covalent hydrogen bonding-based systems with β-cyclodextrin, whereas catechol (PhBcat) and pinacol esters of phenylboronic acid (PhBpin) as well as ferroceneboronic acid (FcBA) form host-guest inclusion complexes. The proposed structural models for the studied complexes are represented in Fig 2.

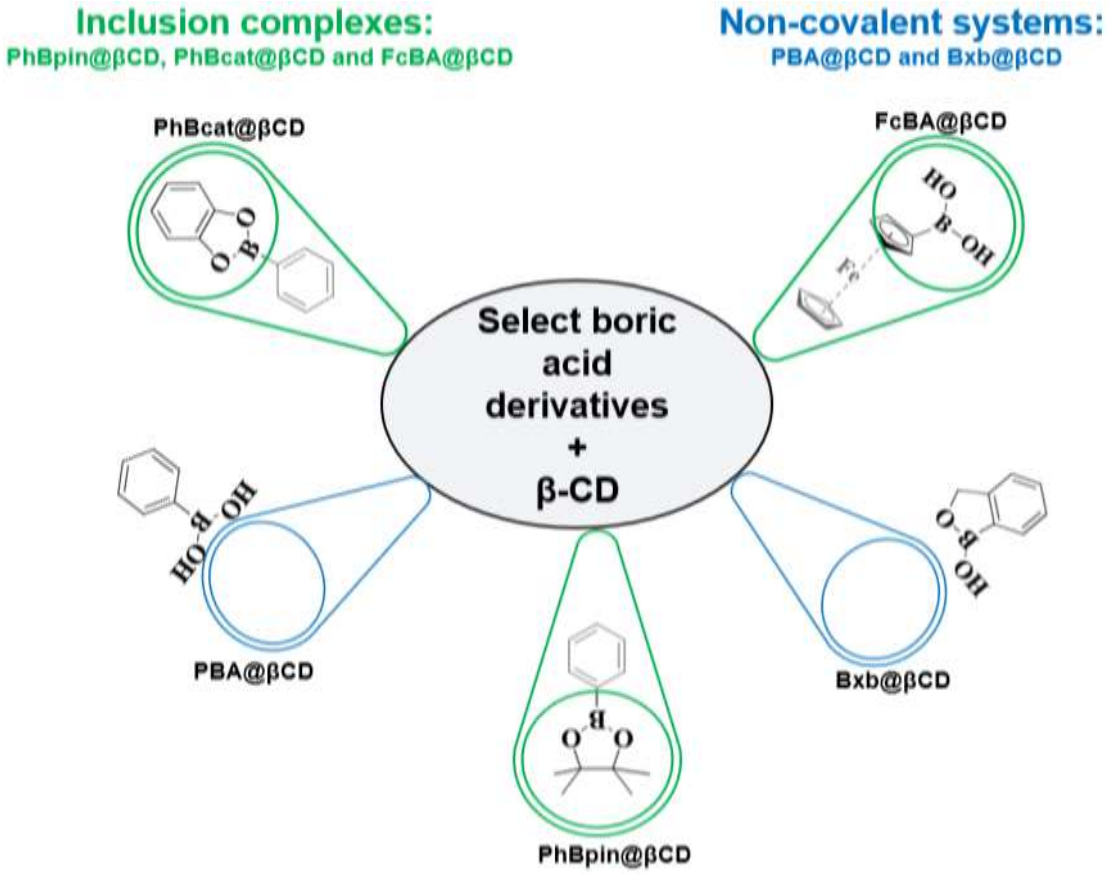

Fig. 2 Interactions of boron-based aromatic systems with β-cyclodextrin **[30]**.

To quantify the interaction between the studied boron-based aromatic systems and β-cyclodextrin, Kasprzak et al. determined the association constant (K_a) of formed complexes. In their study, the experimental association constant follows the trend: FcBa@β-CD (≈ 85 M^{-1}) > PhBcat@β-CD (≈ 46.4) > PBA@β-CD (≈ 42.1) > PhBpin@β-CD (≈ 31.1) > Bxb@β-CD (≈ 14.8). According to the authors, the strength of the K_a is proportional to the number of established hydrogen bonds.

Furthermore, despite the diversity of characterization techniques used, the authors did not explain the mechanism of inclusion. That is why the current study is aimed at a more profound understanding of the inclusion complex formation between select aromatic boron-based compounds (PBA, PhBcat, PhBpin, Bxb and FcBA) and β-CD using density functional theory. To the best of our knowledge, this is the first theoretical study aiming to quantify the interactions between a class of aromatic boron compounds and β-cyclodextrin using exclusively DFT-based calculations.

2. Computational details

DFT-based computations were carried out with ORCA program (version 4.2.0) **[31]** and Gaussian 09 quantum computational package **[32]**. The optimization of the whole inclusion process between select boron compounds and β-CD was performed in vacuum and in water with a conductor-like polarizable continuum model (CPCM) **[33]** at DFT level of theory using BLYP functional in conjunction with Becke-Johnson (BJ) damping function dispersion correction D3(BJ) **[34-38]** and def2-SVP basis set **[39-41]**. For improving the computational efficiency of our large scale calculations, we employed the resolution of the identity (RI) approximation **[42, 43]**.

A geometrical counterpoise correction scheme (gCP) to the def2-SVP for the intra- and inter-molecular basis set superposition error was applied **[44]**. Default values convergence criteria were used for all optimizations. Several studies have shown the reliability of BLYP-D3(BJ) in describing satisfactory non-covalent interactions **[45-48]**.

The natural bond orbital (NBO) calculations were carried out with the Gaussian 09 code in the same manner as the precedent protocol (BLYP-D3(BJ)) but with the larger basis set def2-TZVPP to elucidate the nature of hydrogen bonding in the studied complexes.

The initial structure of β-CD was taken from Chem-Office 3D ultra (Version 10, Cambridge Software) **[49]**. The starting geometries of studied boron compounds were constructed using Hyperchem 7.5 molecular modeling package **[50]**.

The coordinate system defining the process of complexation is represented in Fig. 3.

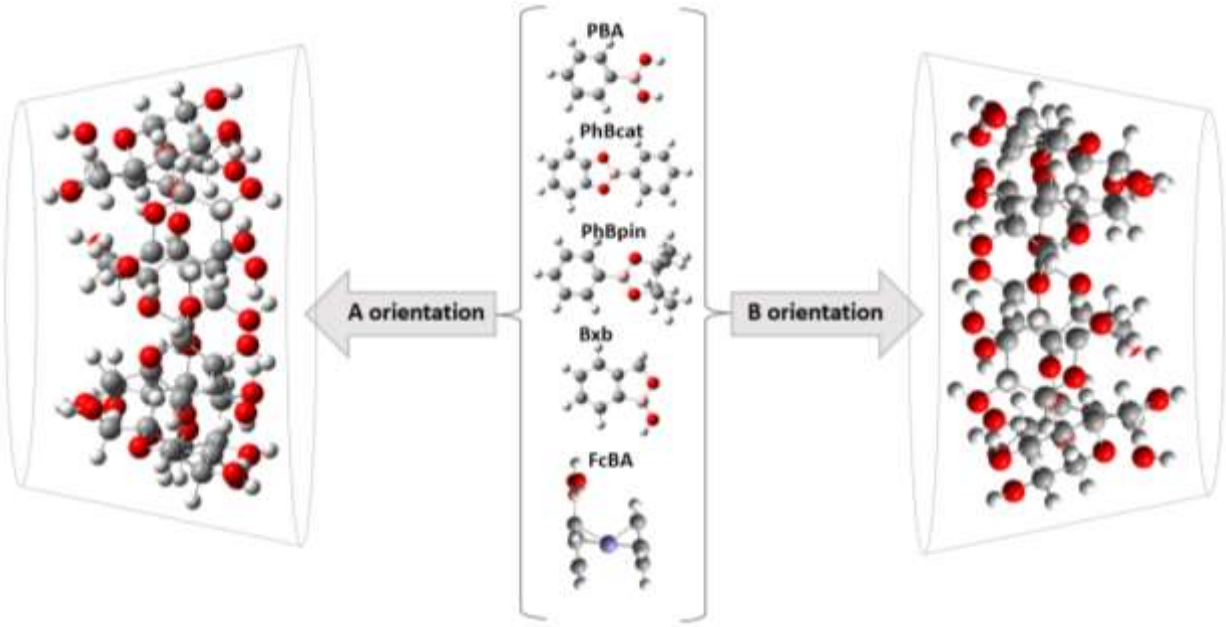

Fig. 3 Coordinate system used to define the inclusion process between studied boron compounds and β-CD. Atom's color code: pink for B, purple for Fe, grey for C, red for O and white for H.

Following the method proposed by Liu and Guo **[51]**, the glycosidic oxygen atoms of β-CD were positioned onto the XY plane; their center was set as the origin of the coordinate system. The secondary hydroxyl groups of the β-CD were placed pointing toward the positive Z-axis. The guest molecules (Aromatic boron compounds) were initially placed at the center of the coordinate system (0 Å), then translated from -5 to +5 Å along the Z-axis in both directions with steps of 1 Å, thus resulting in two possible modes of inclusion A and B (Fig. 3). The structures of guest molecules were initially pre-optimized. All the generated configurations were fully optimized in both gas phase and aqueous solution (CPCM solvent model) at

BLYP-D3/def2-SVP level of theory. The complexation energies for each structure were determined using the following equation:

$$\Delta \boldsymbol{E_{complexation}} = \boldsymbol{E_{guest@\beta-CD}} - (\boldsymbol{E_{guest}} + \boldsymbol{E_{\beta-CD}}) \qquad \textbf{(1)}$$

where $\Delta E_{complexation}$ represent the energy gain due to complexation, $E_{\boldsymbol{guest@\beta-CD}}$, E_{guest} and $E_{\boldsymbol{\beta-CD}}$ are the energies of optimized geometries of the complex, the free guest and the free β-CD, respectively.

For an exploration of the nature and the strength of the interactions **[52-56]** existing between the aromatic boron compounds and β-CD, we performed a reduced density gradient (RDG) **[57]** and independent gradient model (IGM) analysis **[58]**. The non-covalent interactions (NCI) **[59]** maps were characterized with Multiwfn software **[60]** and visualized with VMD program **[61]**, they are represented by generating colored graphs of RDG isosurfaces, where the blue, green and red regions are associated, respectively, to H-bonds, Van der Waals interactions and steric effect.

3. Results and discussion

3.1 Inclusion complexation energy evaluation

The values of the computed complexation energy in gas and aqueous phases as a function of the Z coordinate during the inclusion process for A and B models are reported in Table 1 and 2, where both models exhibit negative energies indicating that the occurring process is thermodynamically favored.

When the guest molecules approach β-CD in gas phase calculations, several local minima were observed, but the most stable geometries based on the lowest complexation energies for PBA@β-CD, PhBcat@β-CD, PhBpin@β-CD, Bxb@β-CD and FcBA@β-CD were located respectively at Z_B = 3.0 Å, Z_A = 1.0 Å, Z_B = -4.0 Å, Z_A = -5.0 Å and Z_A = 0.0 Å and

correspond to the following energies -153.8, -155.5, -172.2, -147.4 and -167.1 kJ/mol (Table 1).

Table 1. Complexation energies (in kJ/mol) of β-CD with aromatic boron compounds calculated in vacuum at BLYP-D3(BJ)/def2-SVP level.

Inclusion mode and related configurations	PBA@β-CD	PhBcat@β-CD	PhBpin@β-CD	Bxb@β-CD	FcBA@β-CD
-5.0A	-143.9	-136.3	-116.1	**-147.4**	-132.0
-4.0A	-127.1	-122.8	-142.3	-141.6	-131.8
-3.0A	-126.8	-144.9	-141.6	-141.4	-153.5
-2.0A	-130.7	-140.3	-148.5	-141.4	-167.1
-1.0A	-130.6	-148.6	-147.6	-135.7	-154.5
0.0A	-120.7	-148.7	-155.0	-129.2	**-167.1**
1.0A	-130.3	**-155.6**	-156.3	-129.2	-141.7
2.0A	-128.1	-133.2	-163.8	-129.2	-127.5
3.0A	-128.2	-145.7	-157.5	-129.2	-131.4
4.0A	-125.6	-134.8	-125.5	-129.4	-155.5
5.0A	-116.6	-121.8	-162.0	-105.4	-150.0
-5.0B	-130.6	-138.4	-140.1	-140.7	-132.5
-4.0B	-125.8	-145.1	**-172.2**	-136.2	-137.9
-3.0B	-145.1	-153.3	-149.4	-135.8	-117.8
-2.0B	-116.6	-147.8	-140.5	-128.2	-132.5
-1.0B	-130.6	-147.5	-140.6	-127.8	-143.0
0.0B	-153.8	-153.3	-142.1	-123.8	-161.0
1.0B	-153.8	-148.5	-142.0	-144.6	-141.9
2.0B	-153.8	-148.5	-136.7	-118.2	-157.0
3.0B	**-153.8**	-128.0	-136.6	-114.2	-153.0
4.0B	-131.3	-143.9	-142.4	-129.8	-164.3
5.0B	-139.1	-129.9	-118.1	-132.4	-164.6

In aqueous phase calculations, the most stable geometries based on the lowest complexation energies for PBA@β-CD, PhBcat@β-CD, PhBpin@β-CD, Bxb@β-CD and FcBA@β-CD were located respectively at Z_B = -2.0 Å, Z_A = 1.0 Å, Z_A = 3.0 Å, Z_A = -1.0 Å and Z_A = -5.0

157 Å and correspond to the following energies -87.0, -96.6, -101.0, -83.8 and -105.3 kJ/mol
158 (Table 2).

159 **Table 2**. Complexation energies (in kJ/mol) of β-CD with aromatic boron compounds
160 calculated in water solvent (cpcm solvation model) at BLYP-D3(BJ)/def2-SVP level.

Inclusion mode and related configurations	PBA@β-CD	PhBcat@β-CD	PhBpin@β-CD	Bxb@β-CD	FcBA@β-CD
-5.0A	-61.5	-77.5	-55.9	-82.9	**-105.3**
-4.0A	-61.0	-76.0	-69.9	-73.6	-103.5
-3.0A	-57.6	-90.0	-75.0	-72.2	-102.4
-2.0A	-51.9	-81.7	-74.1	-82.6	-99.2
-1.0A	-63.2	-79.2	-74.6	**-83.8**	-104.0
0.0A	-72.1	-82.5	-85.8	-53.3	-104.4
1.0A	-61.8	**-96.6**	-88.8	-77.1	-97.2
2.0A	-78.5	-96.5	-71.9	-72.9	-73.5
3.0A	-76.7	-74.6	**-101.0**	-81.0	-95.4
4.0A	-62.8	-62.4	-75.9	-65.9	-95.3
5.0A	-81.1	-75.7	-77.0	-74.2	-66.0
-5.0B	-76.5	-83.7	-94.7	-78.7	-72.1
-4.0B	-77.2	-36.9	-84.8	-69.1	-97.2
-3.0B	-76.7	-81.9	-83.2	-79.2	-71.4
-2.0B	**-87.0**	-87.4	-84.9	-79.1	-58.2
-1.0B	-76.8	-88.3	-83.6	-78.6	-72.2
0.0B	-69.3	-87.1	-83.5	-69.4	-93.7
1.0B	-65.0	-88.7	-83.5	-55.5	-93.9
2.0B	-64.6	-89.2	-74.6	-70.5	-87.9
3.0B	-64.2	-80.3	-81.0	-70.5	-29.2
4.0B	-72.4	-82.9	-73.2	-77.5	-90.5
5.0B	-24.1	-69.7	-54.1	-68.9	-100.8

161

162 The complexation energies are more negative in vacuum than in aqueous solution, they range
163 between -147.4 and -172.2 kJ/mol in gas phase and between -83.8 and -105.2 kJ/mol in water
164 solution. Due to the water solvent effects, the interaction between aromatic boron compounds
165 and β-CD is weakened; showing, therefore, that inclusion process is more exothermic in gas
166 phase than in water.

The calculations carried out in aqueous phase show the same trend towards the complexation energy except that FcBA@β-CD is more stable than PhBpin@β-CD.

It is also observed that complexation energies calculated both in vacuum and in aqueous solution are correlated with the experimental nature of the assembly between the aromatic boron compounds and β-CD. Indeed, the PhBcat@β-CD, PhBpin@β-CD and FcBA@β-CD form inclusion complexes, whereas PBA@β-CD and Bxb@β-CD favor the formation of hydrogen-bonded systems.

The resulting gas phase optimized geometries at BLYP-D3(BJ)/def2-SVP level will be used in the subsequent calculations of NBO and RDG function.

3.2. Theoretical determination of association constant

From a computational viewpoint, the association constant K_a could be calculated according to the following reaction:

$$\beta - CD + guest \xrightarrow{K_a} guest@\beta - CD$$

However, the association constants are determined experimentally in the aqueous phase. To be able to compare the experiment K_a with the results of quantum chemistry calculations, it is, therefore, necessary to take into account the effects of solvation on the calculation of the free reaction enthalpies using CPCM solvent model. It is known that in these types of systems, a continuous model for the solvent can strongly fail since it does not allow evaluating the role of specific interactions between the water molecules and the guest/host molecules. Nevertheless, Champion et al. have proposed a strategy and applied it successfully in predicting reaction equilibrium constants, for instance, for reactions similar to the ones studied in our work **[62, 63]**. They have shown that more accurate results can be obtained when the thermodynamic cycle involves not direct complexation reactions, but rather ligand-exchange reactions by determining the exchange constant K_{exc}. The basic reasoning justifying

the use of this strategy is based on error cancellation mechanisms between the species at the left and the right-hand side.

We hence proceeded accordingly, and, in our calculations, we employed boron compounds exchange reactions involving the guest@βCD species as shown in Fig. 4. We chose the phenylboronic acid catechol (PhBCat) as a reference.

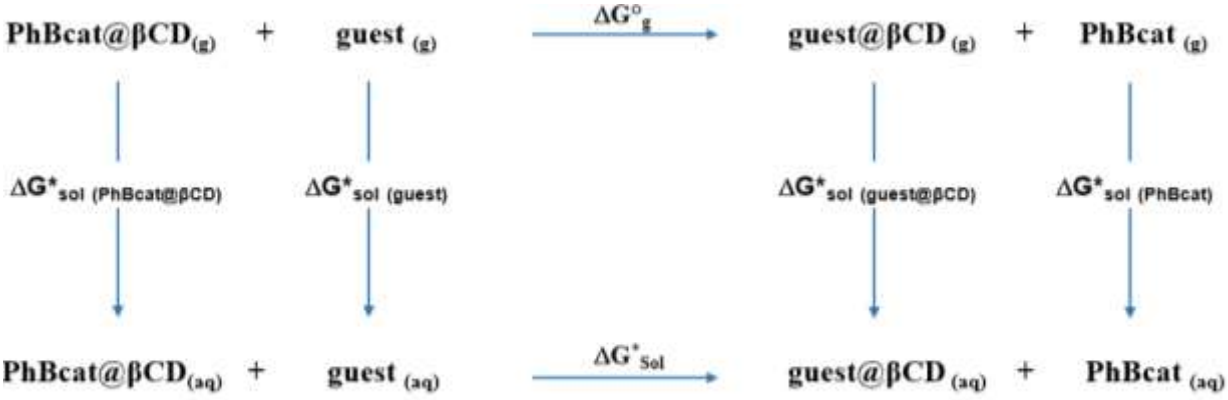

Fig. 4 Thermodynamic cycle used to compute free energy changes in aqueous solution.

The boron compounds exchange equilibrium constant, K_{exc}, is then calculated from the free energy change in aqueous solution, ΔG^*_{Sol}, which can be expressed as:

$$\Delta G^*_{sol} = \Delta G^0_g + \Delta G^*_{sol(guest@\beta-CD)} + \Delta G^*_{sol(PhBcat)} - \Delta G^*_{sol(guest)} - \Delta G^*_{sol(PhBcat@\beta-CD)} \quad (2)$$

Where ΔG^0_g is the free energy change in the gas-phase and $\Delta G^*_{sol\ (guest@\beta CD)}$, $\Delta G^*_{sol\ (PhBcat@\beta CD)}$, $\Delta G^*_{sol\ (guest)}$ and $\Delta G^*_{sol\ (PhBcat)}$ are the free energies of solvation of the respective species in water. For each species, its Gibbs free energy at 25°C is obtained using the computed energy with the BLYP-D3(BJ)/def2-SVP level, and the thermodynamic corrections from the frequency calculation performed with the same functional and basis set in gas-phase. The computed Gibbs free energies at 25°C are regrouped in Table S1. Note that some guests and guest@βCD complexes exhibit several competitive configurations (see, for instance, the case of Bxb@βCD, Fig. S1), their Gibbs free energies have then been evaluated using a Boltzmann distribution:

$$G^{0}_{[A]} = -RT \ln \sum_{i \in [A]} e^{-G^{0}_{i} / RT} \qquad (3)$$

where the summation runs over all the most stable configurations of the A species. The cartesian coordinates of the different configurations used in the determination of the exchange constant are presented in Table S2.

The exchange equilibrium constants (**Log K_{exc}**) computed at the BLYP-D3/def2-SVP level of theory, and the experimental values, are presented in Fig. 5.

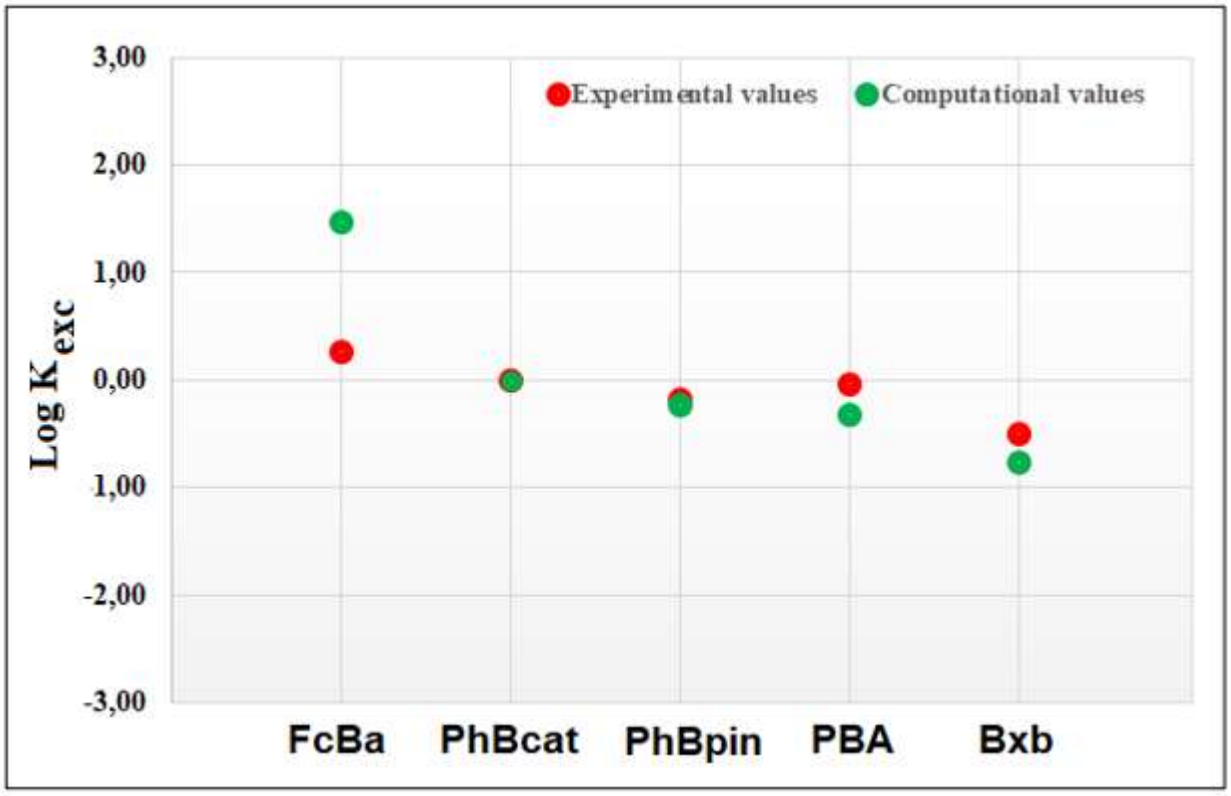

Fig. 5 Correlation of experimental and computational Log K_{exc} values for the studied complexes

From the computed $LogK_{exc}$ (the dots in green color, Fig. 5), it is clear that the complexes PhBcat@β-CD, PhBpin@β-CD and FcBA@β-CD (inclusion complexes) have the three strongest association constants, while the complexes forming hydrogen-bonded systems have the lowest ones. This finding confirms the previous results concerning the complexation energies.

224 On the other hand, we notice that for the FcBA, PhBcat, PhBpin, PBA and Bxb, the
225 computational values agree well with the experimental results. The mean absolute deviation
226 (MAD) between the experimental and computed $LogK_{exc}$ values is rather small (0.37).

227 **3.3. Intermolecular hydrogen-bonding effects**

228 This section is intended to shed light on the ability of the aromatic boron compounds to
229 interact through hydrogen bonds (HBs) with β-CD.
230 NBO method consists in interpreting the electronic wave function in terms of Lewis structures
231 by considering all possible interactions between filled donor (i) and empty acceptor (j) NBOs
232 and evaluating their stabilizing energy through the second-order perturbation theory. The
233 results of NBO analysis associated with the bond length and the stabilization energy of
234 intermolecular hydrogen bonding in the studied complexes are reported in Table 3.
235 A comparison of significant hydrogen bond lengths shows that the values fluctuate between
236 1.85 and 2.76 Å (Fig. 6), the shortest lengths (1.85-2.10 Å) corresponding to strong donor–
237 acceptor interactions **[64, 65]** with higher stabilization energies are associated to the
238 complexes PBA@β-CD, Bxb@β-CD and FcBA@β-CD.
239

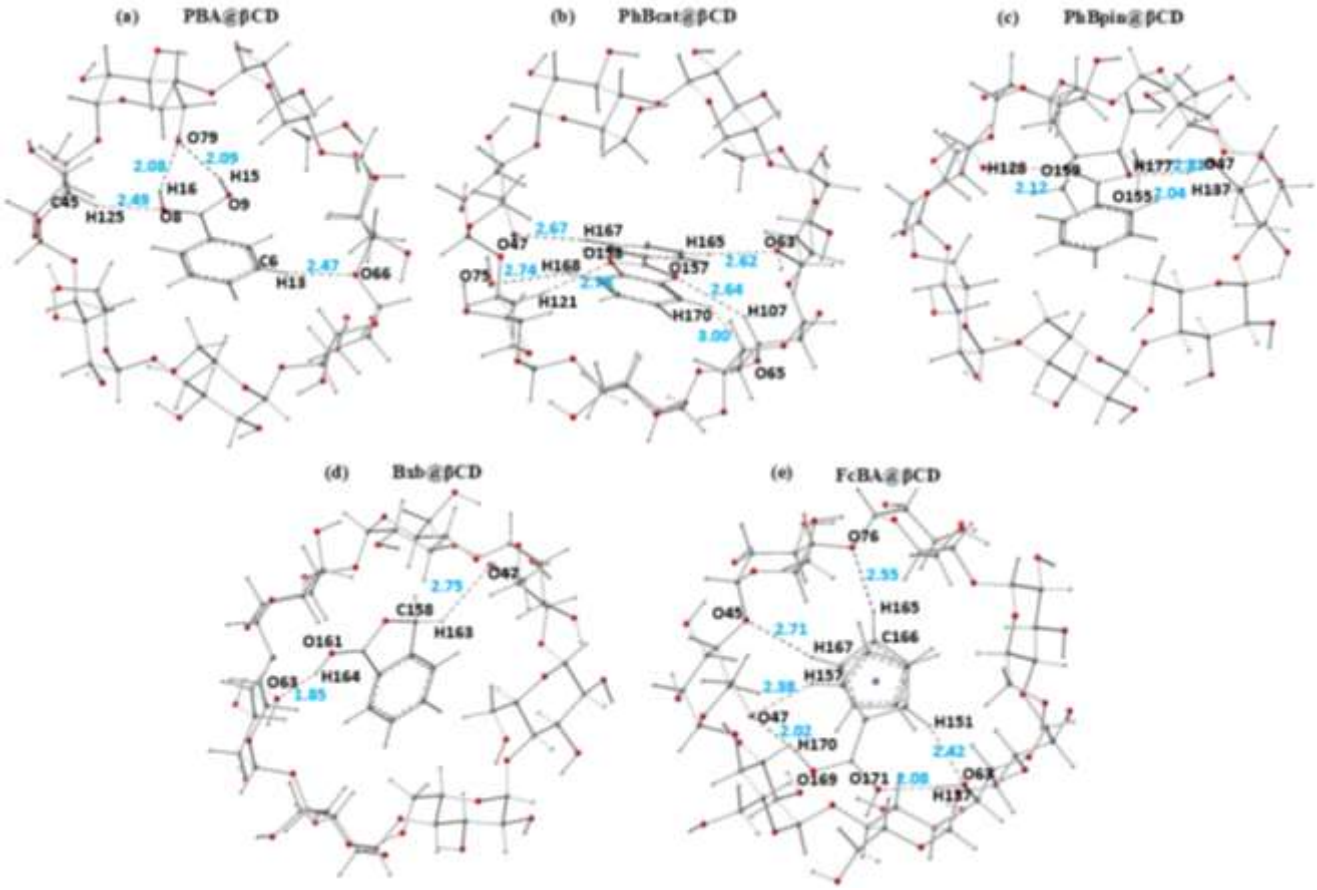

240

241 **Fig. 6** Intermolecular hydrogen bonds illustrated by dashed lines and the corresponding H···O
242 distances (Å). Atom's color code: pink for B, purple for Fe, grey for C, red for O and white
243 for H.

244 The strength of intermolecular hydrogen bonds varies from weak for PhBcat@β-CD and
245 PhBpin@β-CD to moderate for the complexes PBA@β-CD, Bxb@β-CD and FcBA@β-CD.
246 Indeed, as reported in Table 3, the intermolecular hydrogen-bond lengths of PhBcat@β-CD
247 and PhBpin@β-CD complexes are averagely longer than those of PBA@β-CD, Bxb@β-CD
248 and FcBA@β-CD and their corresponding energies are consequently lower.

249

250

251

252

Table 3. NBO analysis of the second-order perturbation energies $E^{(2)}$ (kJ/mol) of the hydrogen bonds in studied complexes calculated at BLYP-D3(BJ)-def2-TZVPP level

Complex	Donor	acceptor	H-bond (Å)	$E^{(2)}$ (kJ/mol)
PBA@β-CD	β-CD (donor)	PBA (acceptor)		
	LP(2) O79	BD*(1) O9-H16	2.08	13.68
	LP(1) O79	BD*(1) O8-H15	2.09	11.97
	LP(1) O79	BD*(1) O9-H16	2.08	4.56
	LP(1) O66	BD*(1) C6-H13	2.47	2.85
	PBA (donor)	β-CD (acceptor)		
	LP(1) O8	BD*(1) C45-H125	2.49	3.31
PhBcat@β-CD	β-CD (donor)	PhBcat (acceptor)		
	LP(2) O47	BD*(1) C155-H167	2.61	2.76
	LP(2) O63	BD*(1) C153-H165	2.62	2.72
	LP(2) O65	BD*(1) C161-H170	3.00	0.92
	LP(2) O75	BD*(1) C159-H168	2.74	1.84
	PhBcat (donor)	β-CD (acceptor)		
	LP(1) O157	BD*(1) C27-H107	2.64	0.92
PhBpin@β-CD	PhBpin (donor)	β-CD (acceptor)		
	LP(1) O155	BD*(1) O63-H137	2.04	14.35
	LP(1) O159	BD*(1) O47-H128	2.12	9.33
	LP(3) O155	BD*(1) O63-H137	2.04	0.92
	β-CD (donor)	PhBpin (acceptor)		
	LP(2) O47	BD*(1) C162-H177	2.81	1.00
Bxb@β-CD	β-CD (donor)	Bxb (acceptor)		
	LP(2) O47	BD*(1) C158-H163	2.75	1.30
	LP(1) O63	BD*(1) O161-H164	1.85	28.74
	LP(2) O63	BD*(1) O161-H164	1.85	6.95
FcBA@β-CD	β-CD (donor)	FcBA (acceptor)		
	LP(1) O47	BD*(1) O169-H170	2.02	11.76
	LP(2) O47	BD*(1) C156-H157	2.38	5.31
	LP(2) O47	BD*(1) O169-H170	2.02	8.45
	LP(2) O63	BD*(1) C150-H151	2.42	5.27
	LP(1) O76	BD*(1) C164-H165	2.55	2.18
	LP(1) O45	BD*(1) C166-H167	2.71	1.21
	FcBA (donor)	β-CD (acceptor)		
	LP(1) O171	BD*(1) O63-H137	2.08	15.77

BD denotes σ bonding orbital; BD* denotes σ* antibonding orbital, LP denotes lone pair.

3.4. Nature of noncovalent interactions

RDG and IGM plots were carried out by an isosurface value of 0.50 and illustrated in Fig. S2 (supplementary data). Red, green and blue colors represent respectively steric repulsion, weak Van der Waals interactions and strong attractive interactions like H-bonds.

The RDG results illustrated in Fig. S2 show clearly that the inclusion of PBA, PhBcat, PhBpin, Bxb and FcBA molecules in β-cyclodextrin exhibited different behavior. The two

guest molecules PhBcat and PhBpin are wrapped by green isosurfaces, indicating weak Van der Waals interactions occurring between the PhBcat and PhBpin molecules and β-CD, whereas for the complexes PBA@β-CD, Bxb@β-CD and FcBA@β-CD, RDG results reveal the presence of weak vdW interactions, as well as the existence of H-bonding interactions involving oxygen atoms of hydroxyl groups (-OH) of PBA, Bxb and FcBA and the hydrogen atoms of OH groups belonging to β-CD, as shown in the circled regions of Fig. S2.

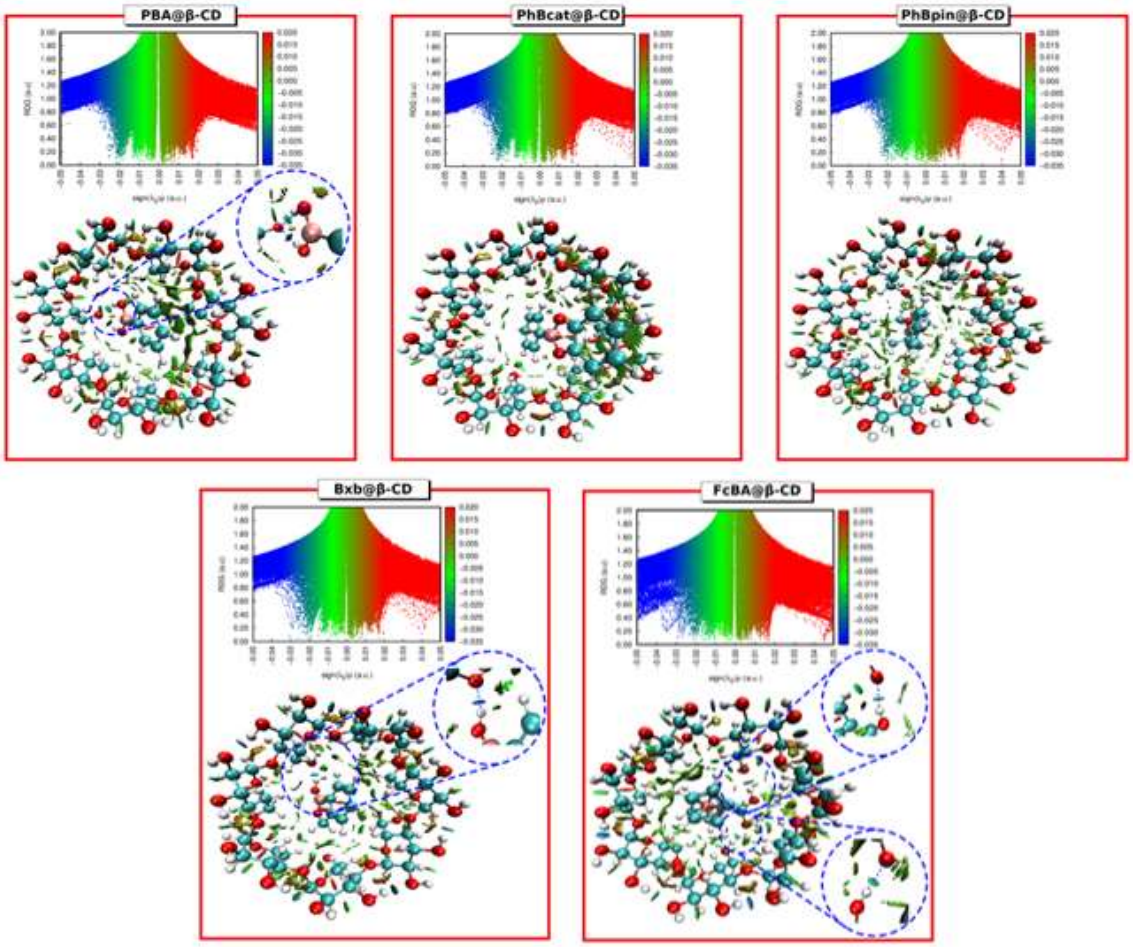

Fig. 7 RDG-isosurfaces of the studied complexes computed at BLYP-D3(BJ) level. Atom's color code: pink for B, purple for Fe, blue for C, red for O and white for H.

Visual inspection of the RDG scatter plots shows the new spikes compared with isolated β-CD (Fig. 7), in the ranges [0.000 to −0.015] and [−0.020 to −0.025] a.u. which correspond respectively, to the vdW and hydrogen bond intermolecular interactions. Additionally, the

intermolecular interactions between β-CD and guest molecules are quantified through the independent gradient model (IGM) to identify the nature of the intermolecular interactions, which can be provided by the δginter and δgintra.

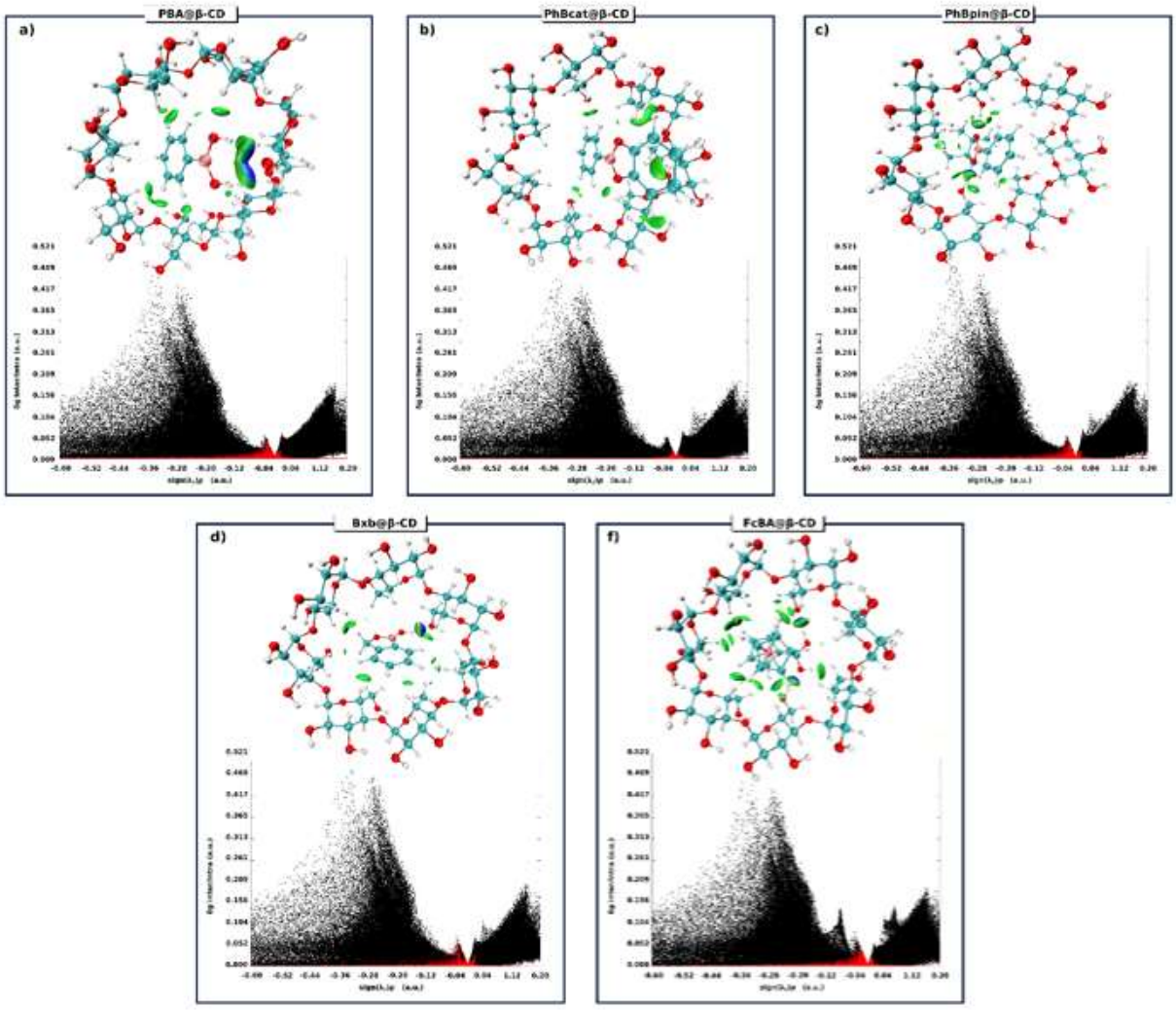

Fig. 8 IGM isosurfaces and scatter plots of the studied complexes. Atom's color code: pink for B, purple for Fe, blue for C, red for O and white for H.

The Fig. 8 represents the IGM isosurfaces of δginter for the five complexes, where the green-colored isosurfaces denote weak van der Waals interactions, whereas blue regions indicate stronger attractive interactions associated with hydrogen bonds.

The scatter plots between δginter and δgintra versus sign(λ2)ρ was shown in lower figures of Fig. 8, in which the red and black points, correspond respectively, to δg^{inter} and δg^{intra}.

The plotted IGM isosurfaces confirmed the nature of occurring interactions. Indeed, the complexes PBA@β-CD and Bxb@β-CD can be considered as hydrogen-bonded complexes, while mainly vdW interactions stabilize PhBcat@β-CD and PhBpin@β-CD. The formation of the complex FcBA@β-CD is a combination of H-bonds and vdW interactions.

Overall, van der Waals (vdW) dispersion interactions strongly affect the stability.

4. Conclusions

In conclusion, we proposed the first DFT study of five systems based on cyclodextrin complexation with a series of aromatic boron compounds. The DFT-D3 investigation results confirmed their experimental ranking based on the formation of inclusion complexes or hydrogen-bonded systems and showed that dispersion interactions are the major contributors to the formation of complexes.

The inclusion process performed in vacuum and in water showed that PhBpin@β-CD and FcBA@β-CD have respectively the highest complexation energies.

The natural bond orbital (NBO), reduced density gradient (RDG) and the independent gradient model (IGM) calculations in gas phase showed that PBA@β-CD and Bxb@β-CD form hydrogen-bonded systems, while mainly vdW interactions stabilize PhBcat@β-CD and PhBpin@β-CD. FcBA@β-CD complex is stabilized by a combination of H-bonds and vdW interactions.

One significant result of this study is the higher stability of ferroceneboronic acid upon its inclusion in the β-cyclodextrin cavity; since ferroceneboronic acid and its derivatives are used as biosensors, this study could serve as a starting point in experiments for overcoming problems of solubility and bioavailability by considering their inclusion in β-cyclodextrin.

*Funding

Not applicable

*Conflicts of interest/Competing interests

Authors declare that they have no financial and/or nonfinancial conflict of interest.

*Availability of data and material

Not applicable

*Code availability

Not applicable

*Authors' contributions

Seyfeddine Rahali: Conceptualization; Formal analysis ; Writing – original draft; Investigation. **Youghourta Belhocine:** Formal analysis ; Software ; review & editing ; Supervision ; Validation. **Hamza Allal:** Methodology ; Software ; Visualization. **Abdelaziz Bouhadiba:** Data curation_ Formal analysis. **Ibtissem Meriem Assabac:** Writing – original draft. **Mahamadou Seydou:** review & editing .

All authors provided critical feedback and helped shape the research, analysis and manuscript.

References

R. Mejia-Ariza, L. Graña-Suárez, W. Verboom and J. Huskens Journal of Materials Chemistry B 5, 1 (2017)
R. Jelinek and S. Kolusheva Chemical reviews 104, 12 (2004)
J.S. Hansen, J.B. Christensen, J.F. Petersen, T. Hoeg-Jensen and J.C. Norrild Sensors and Actuators B: Chemical 161, 1 (2012)
T. Friščić Chemical Society Reviews 41, 9 (2012)
A. Adamczyk-Woźniak, K.M. Borys, K. Czerwińska, B. Gierczyk, M. Jakubczyk, I.D. Madura, A. Sporzyński and E. Tomecka Spectrochimica Acta Part A: Molecular and Biomolecular Spectroscopy 116, (2013)
S.-T. Yang, J. Kim, H.-Y. Cho, S. Kim and W.-S. Ahn RSC advances 2, 27 (2012)
T.J. Jayeoye, W. Cheewasedtham, C. Putson and T. Rujiralai Journal of Molecular Liquids 281, (2019)
H. Geethanjali, R. Melavanki, D. Nagaraja, P. Bhavya and R. Kusanur Journal of Molecular Liquids 227, (2017)

E. Corey Angewandte Chemie International Edition 41, 10 (2002)
E. Dimitrijevic and M.S. Taylor ACS Catalysis 3, 5 (2013)
K. Ishihara Top. Organomet. Chem 49, (2015)
M.S. Taylor Accounts of Chemical Research 48, 2 (2015)
J.A. Peters Coordination Chemistry Reviews 268, (2014)
J. Yan, G. Springsteen, S. Deeter and B. Wang Tetrahedron 60, 49 (2004)
A. Pal, M. Bérubé and D.G. Hall Angewandte Chemie International Edition 49, 8 (2010)
D.G. Hall, Boronic acids: preparation, applications in organic synthesis and medicine, (John Wiley & Sons, 2006)
L. You, D. Zha and E.V. Anslyn Chemical reviews 115, 15 (2015)
J. Wu, B. Kwon, W. Liu, E.V. Anslyn, P. Wang and J.S. Kim Chemical reviews 115, 15 (2015)
T. Gaudisson, S.K. Sharma, R. Mohamed, B.S. Youmbi, N. Menguy, F. Calvayrac, M. Seydou and S. Ammar-Merah CrystEngComm, (2021)
B.C. Das, P. Thapa, R. Karki, C. Schinke, S. Das, S. Kambhampati, S.K. Banerjee, P. Van Veldhuizen, A. Verma and L.M. Weiss Future medicinal chemistry 5, 6 (2013)
P. Chen, Q. Yuan, H. Yang, X. Wen, P. You, D. Hou, J. Xie, Y. Cheng and H. Huang Leukemia Research 57, (2017)
P. dos Passos Menezes, T. de Araújo Andrade, L.A. Frank, G.d.G.G. Trindade, I.A.S. Trindade, M.R. Serafini, S.S. Guterres and A.A. de Souza Araújo International Journal of Pharmaceutics 559, (2019)
V. Bonnet, C. Gervaise, F. Djedaïni-Pilard, A. Furlan and C. Sarazin Drug Discovery Today 20, 9 (2015)
J.M. Casas-Solvas, E. Ortiz-Salmerón, I. Fernández, L. García-Fuentes, F. Santoyo-González and A. Vargas-Berenguel Chemistry–A European Journal 15, 33 (2009)
F. Hapiot, S. Tilloy and E. Monflier Chemical reviews 106, 3 (2006)
A. Harada and S. Takahashi, in Clathrate Compounds, Molecular Inclusion Phenomena, and Cyclodextrins(Springer, 1984), pp. 791-798
A. Harada and S. Takahashi Journal of the Chemical Society, Chemical Communications, 10 (1984)
C. Jullian, S. Miranda, G. Zapata-Torres, F. Mendizábal and C. Olea-Azar Bioorganic & medicinal chemistry 15, 9 (2007)
M. Kompany-Zareh, Z. Mokhtari and H. Abdollahi Chemometrics and Intelligent Laboratory Systems 118, (2012)
A. Kasprzak, K.M. Borys, S. Molchanov and A. Adamczyk-Woźniak Carbohydrate polymers 198, (2018)
F. Neese Wiley Interdisciplinary Reviews: Computational Molecular Science 2, 1 (2012)
M. Frisch, G. Trucks, H.B. Schlegel, G.E. Scuseria, M.A. Robb, J.R. Cheeseman, G. Scalmani, V. Barone, B. Mennucci and G. Petersson Inc., Wallingford CT 201, (2009)
V. Barone and M. Cossi The Journal of Physical Chemistry A 102, 11 (1998)
A.D. Becke Physical review A 38, 6 (1988)
S. Grimme, J. Antony, S. Ehrlich and H. Krieg The Journal of chemical physics 132, 15 (2010)
A.D. Becke and E.R. Johnson The Journal of chemical physics 123, 15 (2005)
E.R. Johnson and A.D. Becke The Journal of chemical physics 124, 17 (2006)
S. Grimme, S. Ehrlich and L. Goerigk Journal of computational chemistry 32, 7 (2011)
A. Schäfer, H. Horn and R. Ahlrichs The Journal of Chemical Physics 97, 4 (1992)
A. Schäfer, C. Huber and R. Ahlrichs The Journal of Chemical Physics 100, 8 (1994)
F. Weigend Physical chemistry chemical physics 8, 9 (2006)
K. Eichkorn, O. Treutler, H. Öhm, M. Häser and R. Ahlrichs Chemical physics letters 240, 4 (1995)
K. Eichkorn, F. Weigend, O. Treutler and R. Ahlrichs Theoretical Chemistry Accounts 97, 1-4 (1997)
H. Kruse and S. Grimme The Journal of chemical physics 136, 15 (2012)
L. Goerigk, A. Hansen, C. Bauer, S. Ehrlich, A. Najibi and S. Grimme Physical Chemistry Chemical Physics 19, 48 (2017)
B. Brauer, M.K. Kesharwani, S. Kozuch and J.M. Martin Physical Chemistry Chemical Physics 18, 31 (2016)
N. Mardirossian and M. Head-Gordon Molecular Physics 115, 19 (2017)
J. Hostas and J. Rezac Journal of Chemical Theory and Computation 13, 8 (2017)

A. Zielesny, (ACS Publications, 2005)
R. Hyperchem Inc, Gainesville, (2002)
L. Liu and Q.-X. Guo Journal of inclusion phenomena and macrocyclic chemistry 50, 1-2 (2004)
J.E.H. Köhler and N. Grczelschak-Mick Beilstein journal of organic chemistry 9, 1 (2013)
A. Bouhadiba, S. Rahali, Y. Belhocine, H. Allal, L. Nouar and M. Rahim Carbohydrate research 491, (2020)
M.I. Sancho, S. Andujar, R.D. Porasso and R.D. Enriz The Journal of Physical Chemistry B 120, 12 (2016)
D. Zhang, J. Liu, T. Wang and L. Sun Journal of molecular modeling 23, 4 (2017)
Y.-Z. Yang, X.-F. Liu, R.-b. Zhang and S.-P. Pang Physical Chemistry Chemical Physics 19, 46 (2017)
G. Saleh, C. Gatti and L.L. Presti Computational and Theoretical Chemistry 998, (2012)
C. Lefebvre, H. Khartabil, J.C. Boisson, J. Contreras-García, J.P. Piquemal and E. Hénon ChemPhysChem 19, 6 (2018)
J. Contreras-García, R.A. Boto, F. Izquierdo-Ruiz, I. Reva, T. Woller and M. Alonso Theoretical Chemistry Accounts 135, 10 (2016)
T. Lu and F. Chen Journal of computational chemistry 33, 5 (2012)
W. Humphrey, A. Dalke and K. Schulten Journal of molecular graphics 14, 1 (1996)
J. Champion, M. Seydou, A. Sabatié-Gogova, E. Renault, G. Montavon and N. Galland Physical Chemistry Chemical Physics 13, 33 (2011)
J. Champion, A. Sabatie-Gogova, F. Bassal, T. Ayed, C. Alliot, N. Galland and G. Montavon The Journal of Physical Chemistry A 117, 9 (2013)
I.M. Assaba, S. Rahali, Y. Belhocine and H. Allal Journal of Molecular Structure, (2020)
I. Djilani and D.E. Khatmic,

Figures

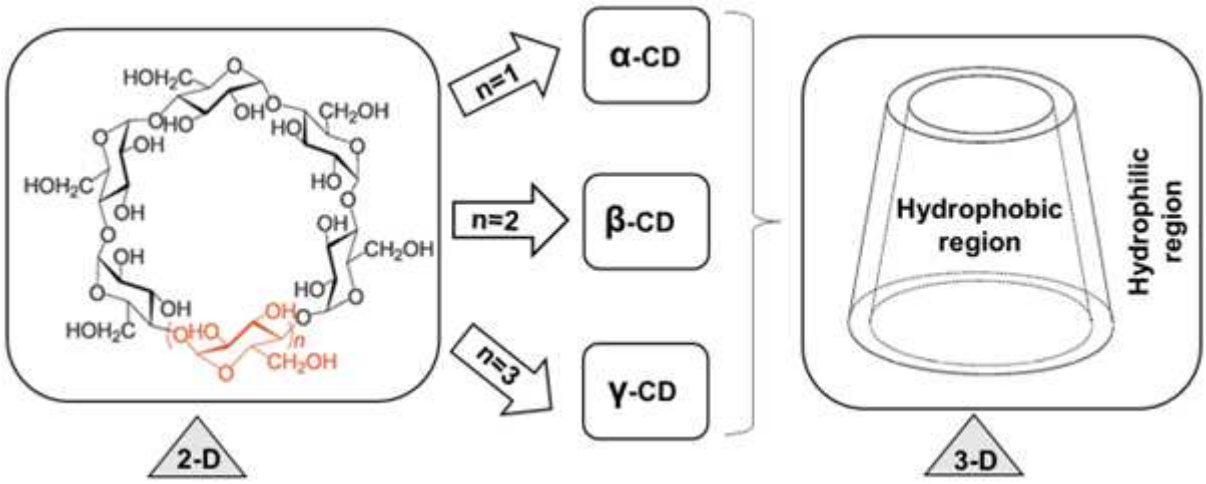

Figure 1

Chemical structure and 3D-model of cyclodextrins.

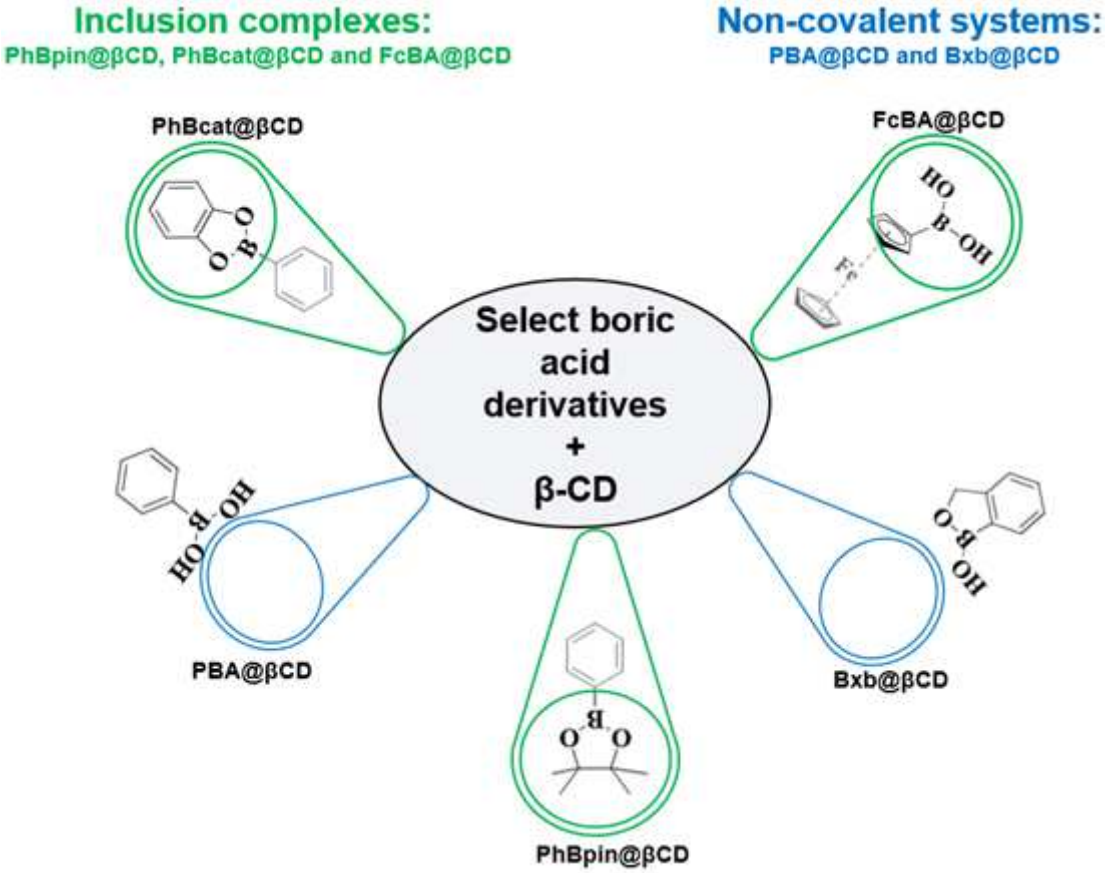

Figure 2

Interactions of boron-based aromatic systems with β-cyclodextrin [30].

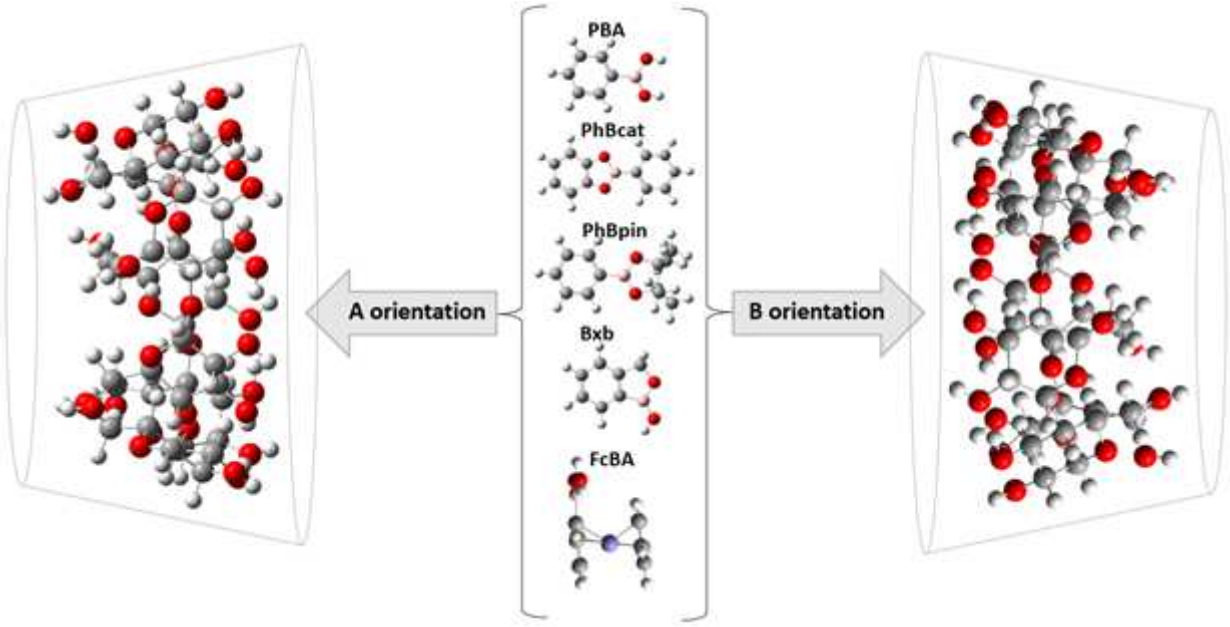

Figure 3

Coordinate system used to define the inclusion process between studied boron compounds and β-CD. Atom's color code: pink for B, purple for Fe, grey for C, red for O and white for H.

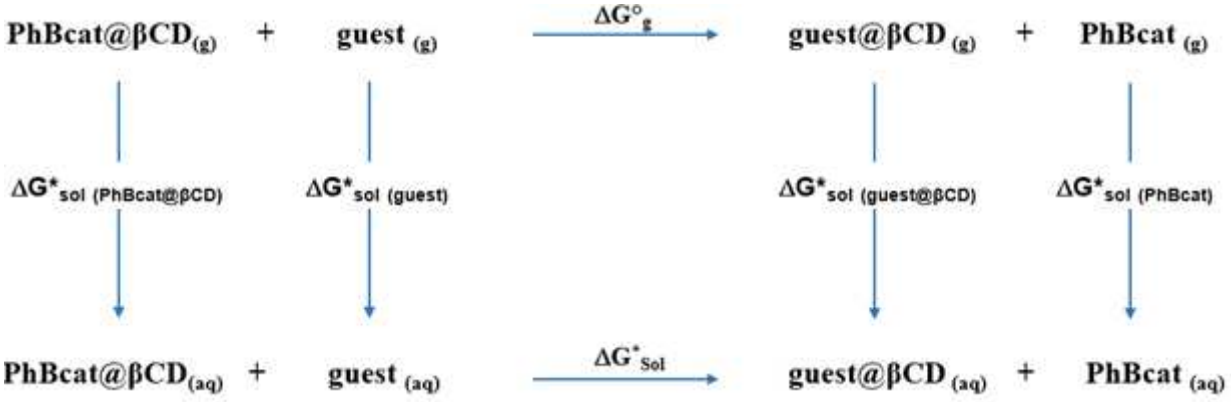

Figure 4

Thermodynamic cycle used to compute free energy changes in aqueous solution.

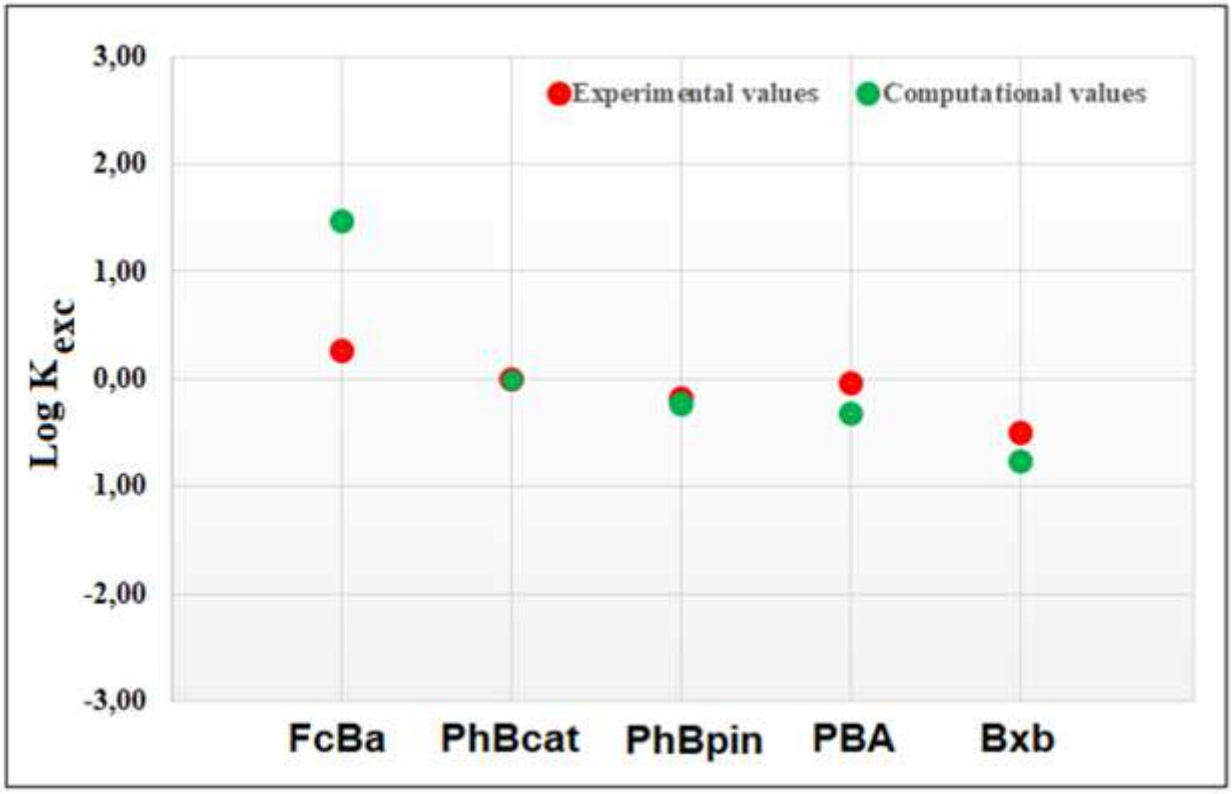

Figure 5

Correlation of experimental and computational Log Kexc values for the studied complexes

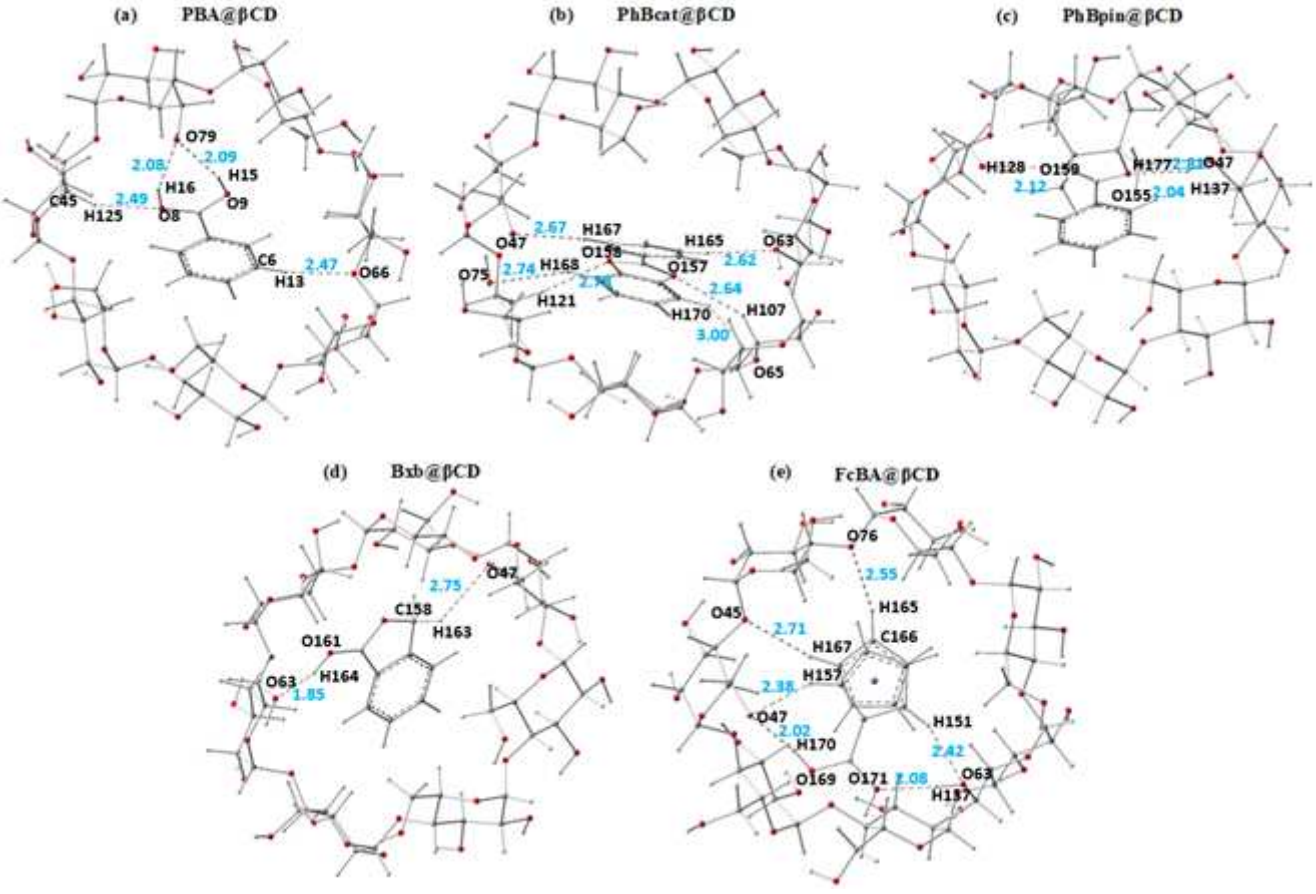

Figure 6

Intermolecular hydrogen bonds illustrated by dashed lines and the corresponding H···O distances (Å). Atom's color code: pink for B, purple for Fe, grey for C, red for O and white for H.

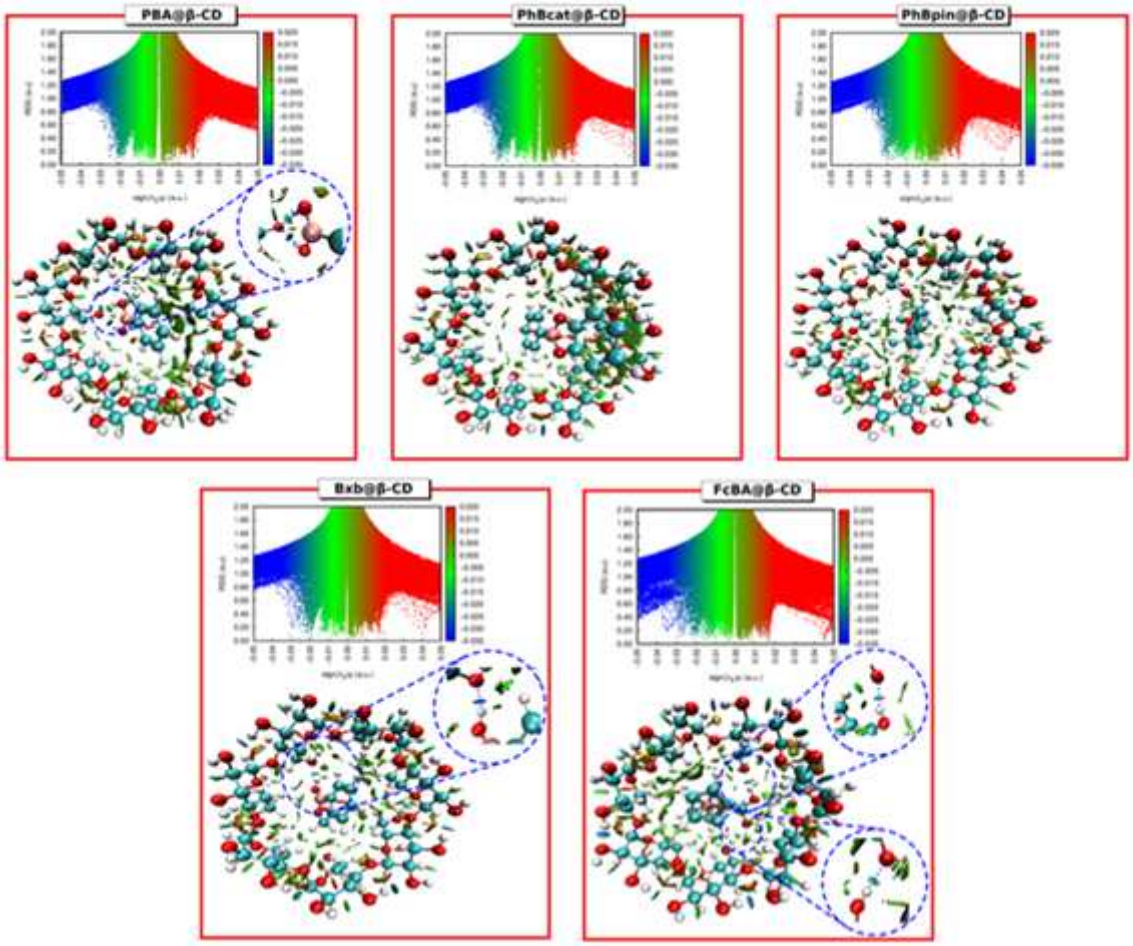

Figure 7

RDG-isosurfaces of the studied complexes computed at BLYP-D3(BJ) level. Atom's color code: pink for B, purple for Fe, blue for C, red for O and white for H.

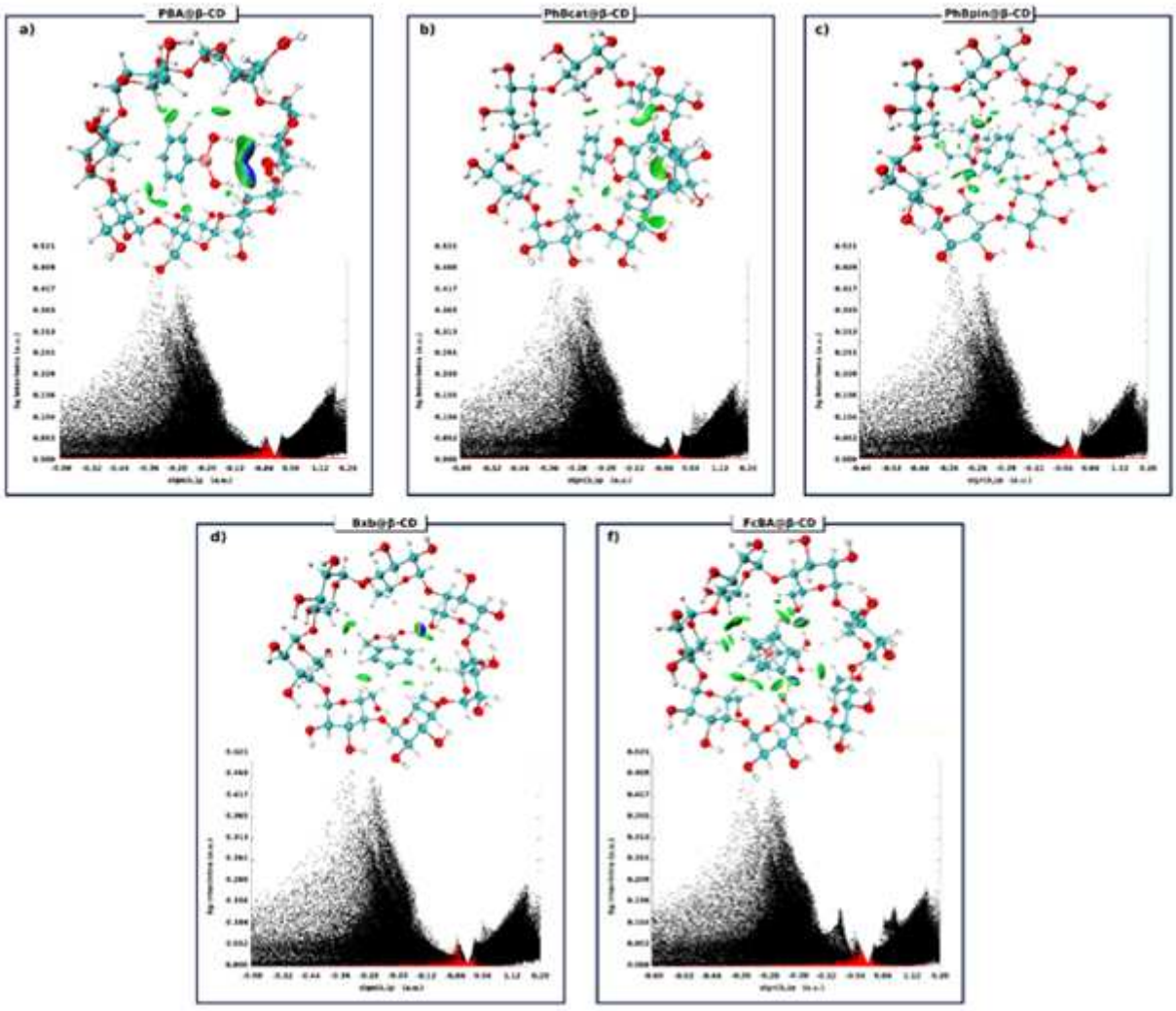

Figure 8

IGM isosurfaces and scatter plots of the studied complexes. Atom's color code: pink for B, purple for Fe, blue for C, red for O and white for H.

Supplementary Files

This is a list of supplementary files associated with this preprint. Click to download.

- Supplementarydata.docx